

Generating Periodic Motions for the Butterfly Robot

Daniel Ortíz Morales*, Pedro La Hera†, and Shafiq Ur Réhman*.

Abstract—We analyze the problem of dynamic non-prehensile manipulation by considering the example of the butterfly robot. Our main objective is to study the problem of stabilizing periodic motions, which resemble some form of juggling acrobatics. To this end, we approach the problem by considering the framework of virtual holonomic constraints. Under this basis, we provide an analytical and systematic solution to the problems of trajectory planning and design of feedback controllers to guarantee orbital exponential stability. Results are presented in the form of simulation tests.

Index Terms—Underactuated mechanical systems, limit cycles, virtual holonomic constraints, transverse linearization.

I. INTRODUCTION

Mechanical devices with fewer control inputs than degrees of freedom, also known as underactuated systems, are standard tools for developing and testing nonlinear control methods. One of these examples is the Butterfly system, which was introduced by K. Lynch [1] to understand the problem of dynamical manipulation in the form of robotic juggling.

The Butterfly robot consists of two plates coupled to form a track where a ball freely moves, as it is depicted in Fig. 1. This coupling is actuated at its center by an electric motor, while the ball has constrained movement due to contact, but it is not actively actuated in any form. It is a two degree of freedom (d.o.f) mechanical system, these d.o.f. are the angle of the plates and the angle of the ball. One of the many interesting challenges allocated to this setup is the generation of periodic juggling-like motions at different equilibrium points. To the best of our knowledge, two approaches have been proposed: 1) optimization-based motion planning under PD feedback control [1] and 2) passivity based control [2], [3]. Within this context, our aim is to present a dedicated study based on the virtual holonomic constraints (VHC) approach [4], [5], which is a method that has proven to be useful for deriving analytical solutions to similar problems. Our motivation lays on the analytical and experimental success achieved in various underactuated mechanical systems, such as the cart pendulum [6], pendubot [7], [8], Furuta pendulum [9], inertial wheel pendulum [10], biped robots [11], [12], [13], magnetic levitator [14], etc. Our main contribution is the application of the VHC theory to achieve periodic motions at different equilibrium points of the butterfly robot.

*D.Ortíz Morales and S. Ur Réhman work at the Department of Applied Physics and Electronics, Umeå University, Sweden, 90187, daniel.ortiz.morales@umu.se, shafiq.urrehman@umu.se

†P. La Hera works at the Department of Forest Technology, Swedish University of Agricultural Sciences, Sweden, 90183, xavier.lahera@slu.se

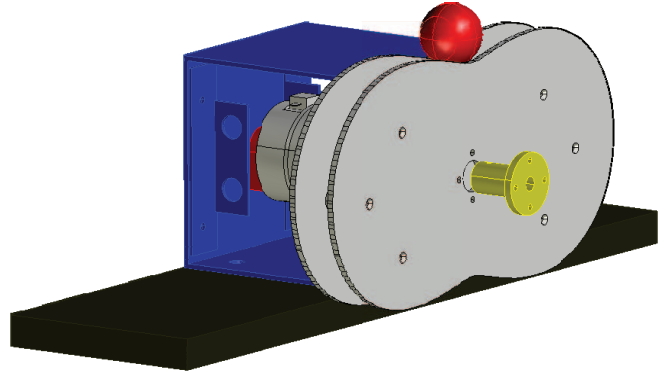


Fig. 1: Butterfly robot. CAD-drawing courtesy of M. Cefalo, University of Rome "La Sapienza"

II. MODEL OF THE BUTTERFLY ROBOT

The generalized coordinates are defined by the vector $q = [q_1, q_2]^T$, where q_1 and q_2 denote the angular positions of the plates and ball w.r.t. to the horizontal and vertical axis of the world frame respectively, see Fig. 2. Under the assumption of sliding contact between the ball and the plates, dynamics of the system can be approximated by the standard second order Euler-Lagrange model [15]:

$$M(q)\ddot{q} + C(q, \dot{q})\dot{q} + G(q) = \begin{bmatrix} u \\ 0 \end{bmatrix}, \quad (1)$$

where $M(q)$ denotes the inertia matrix, $C(q, \dot{q})$ the matrix of Coriolis and centrifugal forces, $G(q)$ the vector of gravity, and u the input acting on the plates of the Butterfly. The expressions for these matrices are given below

$$M(q) = \begin{bmatrix} J + m_b \delta^2 & -m_b \delta^2 \\ -m_b \delta^2 & m_b (\delta'^2 + \delta^2) \end{bmatrix} \quad (2)$$

$$C(q, \dot{q}) = m_b \delta' \begin{bmatrix} \delta \dot{q}_2 & \delta (\dot{q}_1 - 2 \dot{q}_2) \\ -\delta \dot{q}_1 & \dot{q}_2 (\delta + \delta'') \end{bmatrix} \quad (3)$$

$$G(q) = m_b g \begin{bmatrix} -\delta \sin(q_1 - q_2) \\ \delta' \cos(q_1 - q_2) + \delta \sin(q_1 - q_2) \end{bmatrix} \quad (4)$$

where J is the moment of inertia of the rotational link, m_b is the ball mass, g is the constant of gravity, and $\delta := \delta(q_2)$ is the distance from the center of the ball to the rotational axis of the joint, and

$$\delta' = \frac{\partial \delta(q_2)}{\partial q_2}, \quad \delta'' = \frac{\partial^2 \delta(q_2)}{\partial q_2^2}. \quad (5)$$

Considering the model developed by M. Cefalo [2], [3], one possible geometrical shape for the plates can be calculated by the following expressions

$$\begin{aligned} x_c(s) &= 14.9 - 25s^2 + 10.1s^4, \\ y_c(s) &= -19.9s + 23.3s^3 - 10s^5, \end{aligned} \quad (6)$$

in which $s \in [-1, 1]$. These polynomials (6) describe the right half of the contour, and the left half is defined by symmetry, i.e. $-x_c(s)$. As shown in Fig. 2, the Cartesian coordinates of the ball's center of gravity relative to the Butterfly's contour are given by

$$\begin{aligned} x_b(s) &= -r_{eq} \sin \left(\arctan \left(\frac{\partial y_c(s)}{\partial x_c(s)} \right) \right), \\ y_b(s) &= r_{eq} \cos \left(\arctan \left(\frac{\partial y_c(s)}{\partial x_c(s)} \right) \right), \end{aligned} \quad (7)$$

where $\frac{\partial y_c(s)}{\partial x_c(s)}$ is the rate of change of the Cartesian coordinates with respect to the parameterizing variable s , and r_{eq} is the distance between the center of the ball to the contact point with the plates, and it is given by:

$$r_{eq} = r \cos(\xi), \quad \xi = \arcsin \left(\frac{l}{2r} \right), \quad (8)$$

where r is the radius of the ball, and l is the distance between the plates. The coordinates of the center of the ball with

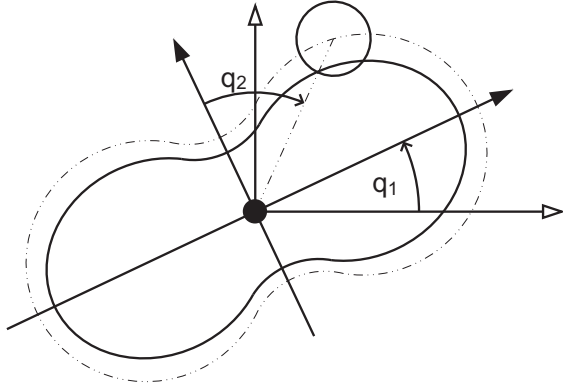


Fig. 2: Generalized coordinates of the Butterfly robot. The black shape is the boundary of the plates, and the dashed line shows all possible Cartesian coordinates of the ball's center of gravity around the Butterfly contour, provided that contact is ensured.

respect to the center of the plates are:

$$\begin{aligned} x(s) &= x_c(s) + x_b(s), \\ y(s) &= y_c(s) + y_b(s). \end{aligned} \quad (9)$$

Hence, the distance from the center of the robot to the center

TABLE I: Physical parameters of the butterfly robot

Parameters	Value [units]
m_b	0.02 [Kg]
J	0.0509455 [Kg · m ²]
r	0.017 [m]
l	0.0230 [m]
r_{eq}	0.0115 [m]
g	9.81 [m/sec ²]

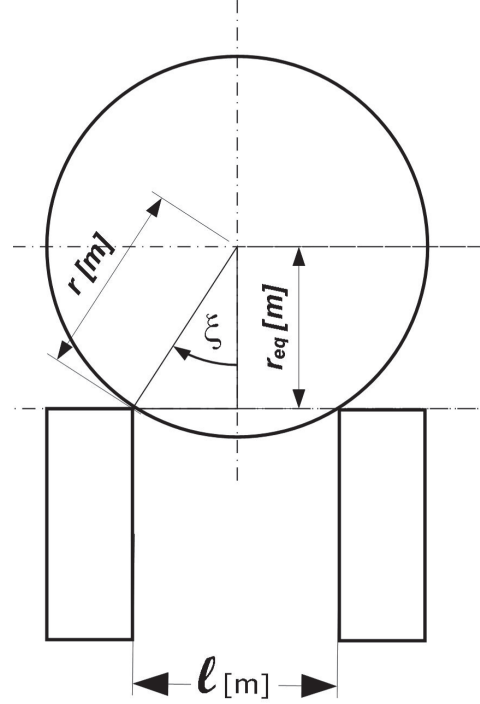


Fig. 3: Distance from the contact point between the center of ball and the boundary of the shape

of the ball and the angle q_2 are given by

$$\delta(s) = \sqrt{x(s)^2 + y(s)^2}, \quad q_2(s) = \arctan \left(\frac{x(s)}{y(s)} \right). \quad (10)$$

A. Reaction Force

In order to calculate the reaction forces at the contact point, we consider an extended second order system [13]

$$M_e(q_e)\ddot{q}_e + C_e(q_e, \dot{q}_e)\dot{q}_e + G_e(q_e) = \begin{bmatrix} u \\ 0 \\ F_T \\ F_N \end{bmatrix}, \quad (11)$$

where $q_e := (q_1, q_2, x, y)^T$ is an extended set of generalized coordinates, $[F_T, F_N]$ are the tangential and normal force between the ball and the plates. The normal force can be used to validate whether or not a motion is feasible, given that the inequality

$$F_N > 0, \quad (12)$$

is satisfied at all times.

III. TRAJECTORY PLANNING

Any trajectory $q(t)$ can be represented as the time evolution of the generalized coordinates and denoted as:

$$q = \begin{bmatrix} q_1 \\ q_2 \end{bmatrix} = \begin{bmatrix} q_{1*}(t) \\ q_{2*}(t) \end{bmatrix}. \quad (13)$$

An alternative parametric representation of the same motion can also be given as

$$\begin{bmatrix} q_1 \\ q_2 \end{bmatrix} = \begin{bmatrix} \theta_*(t) \\ \phi(\theta_*(t)) \end{bmatrix}, \quad (14)$$

where the motion is described in terms of a virtual holonomic constraint given by the function $\phi(\cdot)$, according to the evolution of $\theta_* \in [\Theta_b, \Theta_e]$. Thus, in a general form (14) can be written as

$$\begin{bmatrix} q_1 \\ q_2 \end{bmatrix} = \begin{bmatrix} \theta \\ \phi(\theta) \end{bmatrix}, \quad (15)$$

where the explicit dependence of time disappears, and θ becomes the trajectory generator. Dynamics (1) in terms of θ can also be found by substituting the time derivatives

$$\begin{bmatrix} \dot{q}_1 \\ \dot{q}_2 \end{bmatrix} = \begin{bmatrix} \dot{\theta} \\ \phi'(\theta)\dot{\theta} \end{bmatrix}, \quad \begin{bmatrix} \ddot{q}_1 \\ \ddot{q}_2 \end{bmatrix} = \begin{bmatrix} \ddot{\theta} \\ \phi''(\theta)\dot{\theta}^2 + \phi'(\theta)\ddot{\theta} \end{bmatrix}, \quad (16)$$

into the dynamics model (1), which yields a set of differential equations of the form:

$$\alpha_1(\theta)\ddot{\theta} + \beta_1(\theta)\dot{\theta}^2 + \gamma_1(\theta) = u, \quad (17)$$

$$\alpha_2(\theta)\ddot{\theta} + \beta_2(\theta)\dot{\theta}^2 + \gamma_2(\theta) = 0, \quad (18)$$

also known as the reduced dynamics. For the particular unactuated dynamics (18) these expressions are¹:

$$\begin{aligned} \alpha_2(\theta) &= -m_b \left[(-\delta'^2 - \delta^2) \phi'(\theta) + \delta^2 \right], \\ \beta_2(\theta) &= m_b \left[\phi''(\theta) (\delta'^2 + \delta^2) + \phi'(\theta)^2 \delta' (\delta + \delta'') \right. \\ &\quad \left. - \delta \delta' \right], \\ \gamma_2(\theta) &= m_b g [\delta' \cos(\theta - \phi(\theta)) + \delta \sin(\theta - \phi(\theta))]. \end{aligned} \quad (19)$$

It is being demonstrated in [5] that trajectories of the system (1) can be found by solving (18) given a set of initial conditions $[\theta_0, \dot{\theta}_0]$, and the constraint function (15). This is also valid for periodic motions, which are also solutions of (18) that fulfill a number of conditions. These conditions are presented below, for which we refer to the analytical demonstrations in [5].

IV. EXAMPLES OF CONSTRAINT FUNCTIONS

In order to exemplify our procedure, let us consider two different constraint functions, with the equilibrium (θ_0, ϕ_0) pointing at the center of different periodic cycles:

$$\phi_1(\theta) = k_1 \cdot \arctan(\theta - \theta_0) + \phi_0, \quad (20)$$

$$\phi_2(\theta) = k_2(\theta - \theta_0) + \phi_0, \quad (21)$$

such that the angular movement of the ball q_2 is limited by the constants k_1 and k_2 , irrespective of the trajectory of the actuated joint. The problem of trajectory planning consists on finding the values of k_1 and k_2 for which the solutions of (18) yield a periodic response. To exemplify the procedure

¹The distance $\delta(q_2)$ is now expressed in terms of $\delta(\phi(\theta))$, to simplify the notation this term is denoted simply by δ .

of how to choose these values, we consider the case of two different equilibriums, i.e.

- 1) *Equilibrium 1.* When the Butterfly plates are in the horizontal position, thus

$$\theta_0 = 0 \quad \phi_0 = 0. \quad (22)$$

- 2) *Equilibrium 2.* When the Butterfly plates are in the vertical position.

$$\theta_0 = \frac{\pi}{2} \quad \phi_0 = \frac{\pi}{2}. \quad (23)$$

We also recall the following lemma extracted from [5].

Lemma 1: The existence of periodic solutions for the system (18) is guaranteed provided that:

$$\omega^2 = \frac{\gamma_2'(\theta_0)}{\alpha_2(\theta_0)} > 0, \quad (24)$$

for which the derivative of the function $\gamma_2(\theta)$ with respect to θ , yields

$$\begin{aligned} \gamma_2'(\theta) &= m_b g [\delta'' \phi'(\theta) \cos(\theta - \phi(\theta)) + \\ &\quad + \delta' \sin(\theta - \phi(\theta)) (2 \phi'(\theta) - 1) \\ &\quad + \delta \cos(\theta - \phi(\theta)) (1 - \phi'(\theta))]. \end{aligned} \quad (25)$$

1) *Arctangent constraint:* Considering (20), the partial derivatives of this constraint function are:

$$\phi_1'(\theta) = \frac{k_1}{1 + (\theta - \theta_0)^2}, \quad (26)$$

$$\phi_1''(\theta) = -\frac{2k_1(\theta - \theta_0)}{(1 + (\theta - \theta_0)^2)^2}, \quad (27)$$

Therefore, evaluating (20), (26) and (27) at the equilibrium (22) we obtain

$$\phi_1(\theta_0) = 0, \quad \phi_1'(\theta_0) = k_1, \quad \phi_1''(\theta_0) = 0. \quad (28)$$

Solving the inequality (24), using (28), yields that

$$\omega^2 = -g \frac{\delta''(0) k_1 + \delta(0)(1 - k_1)}{[-\delta'(0)^2 - \delta(0)^2] k_1 + \delta(0)^2} > 0, \quad (29)$$

which allows to find the interval where k_1 guarantees the existence of periodic solutions:

$$-0.8684 < k_1 \vee k_1 > 1 \quad (30)$$

As an example, the solutions of (18) with $k_1 = 1.5$ and different initial conditions for $[\theta, \dot{\theta}]$ are shown in Fig.4

2) *Linear constraint:* The partial derivatives of this type of constraint are:

$$\phi_2'(\theta) = k_2, \quad (31)$$

$$\phi_2''(\theta) = 0. \quad (32)$$

It is clear that the functions above remain constant whenever they are evaluated in any equilibrium, i.e. $\theta = \theta_0$ and $\phi_2(\theta_0) = \phi_0$. Analyzing the periodicity condition (24) of the system (18) in the vertical equilibrium (23) i.e.

$$\omega^2 = -g \frac{\delta''(\frac{\pi}{2}) k_2 + \delta(\frac{\pi}{2})(1 - k_2)}{[-\delta'(\frac{\pi}{2})^2 - \delta(\frac{\pi}{2})^2] k_2 + \delta(\frac{\pi}{2})^2} > 0, \quad (33)$$

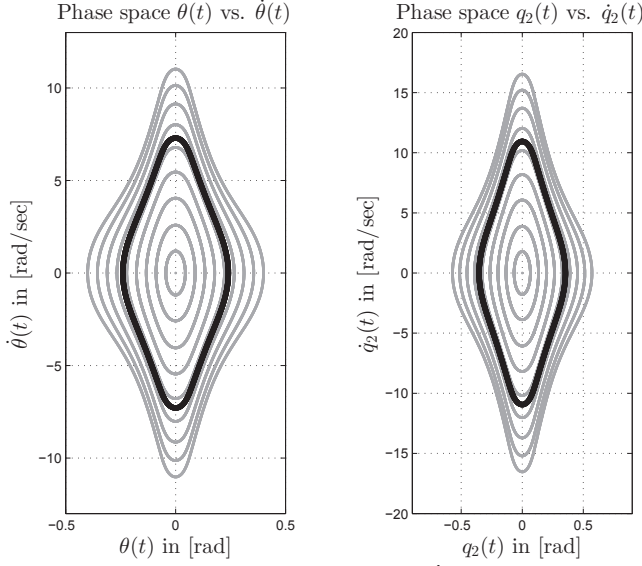


Fig. 4: Left: Phase-Space of (18), θ vs $\dot{\theta}$ using an arctangent constraint. Right: Phase-Space of q_2 vs \dot{q}_2 . The bold line represents the orbit analyzed for simulations in section VI. The direction of motion for θ is clockwise.

yields the interval where k_2 produces periodic solutions, i.e.

$$0.61 < k_2 < 1 \quad (34)$$

Solving (18) with $k_2 = 0.87$ and different initial conditions for $[\theta, \dot{\theta}]$ are shown in Fig.5

V. CONTROL DESIGN

Our control design techniques is based on the work of [16], [17], [18], which proposes the use of transverse coordinates for the design of feedback controllers.

A. Dynamics along the target orbit and transverse coordinates

A given motion of the mechanical system (1), in the form (15), allows to introduce a vector of new generalized coordinates in the vicinity of the orbit, i.e.

$$\begin{bmatrix} \theta \\ Y \end{bmatrix} = \begin{bmatrix} q_1 \\ q_2 - \phi(\theta) \end{bmatrix}, \quad (35)$$

with its time derivative being

$$\begin{bmatrix} \dot{\theta} \\ \dot{Y} \end{bmatrix} = \begin{bmatrix} \dot{q}_1 \\ \dot{q}_2 - \phi'(\theta)\dot{\theta} \end{bmatrix}. \quad (36)$$

The purpose of the control action is to exponentially drive the response of the system (1) to the solution

$$\theta = \theta_*(t), \quad \dot{\theta} = \dot{\theta}_*(t), \quad Y = 0, \quad \dot{Y} = 0, \quad (37)$$

from any given initial condition, and for $t > 0$. Dynamics (1) in the new coordinates can be found by introducing (35), (36), and

$$\begin{bmatrix} \ddot{\theta} \\ \ddot{Y} \end{bmatrix} = \begin{bmatrix} \ddot{q}_1 \\ \ddot{q}_2 - (\phi''(\theta)\dot{\theta}^2 + \phi'(\theta)\ddot{\theta}) \end{bmatrix}, \quad (38)$$

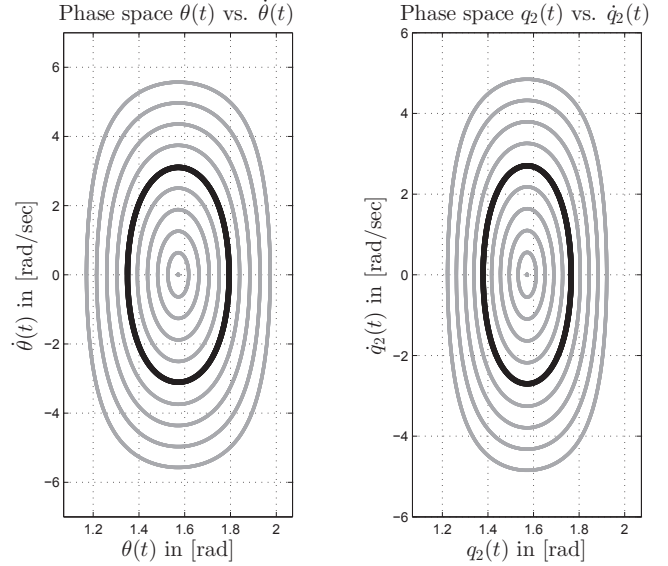


Fig. 5: Left: Phase-Space of (18), θ vs $\dot{\theta}$ using a linear constraint. Right: Phase-Space of q_2 vs \dot{q}_2 . The bold line represents the orbit analyzed for simulations in section VI. The direction of motion for θ is clockwise.

into dynamics of the robot (1). This substitution yields the dynamic model:

$$R(\theta, Y, \dot{\theta}, \dot{Y}) + N(\theta, Y)u = \ddot{Y}, \quad (39)$$

$$\alpha_2(\theta)\ddot{\theta} + \beta_2(\theta)\dot{\theta}^2 + \gamma_2(\theta) = g_i(\theta, \dot{\theta}, Y, \dot{Y}, \ddot{Y}). \quad (40)$$

where $g_i(\cdot)$ is a smooth function that is equal to zero on the desired orbit.

B. Partial feedback linearization

Introducing the feedback transformation

$$u = \frac{1}{N} v - \frac{R}{N}, \quad (41)$$

with $N(\theta_*(t), 0) \neq 0$ for all $t \in [0, T_e]$, brings the Y -dynamics (40) into the linear form $\ddot{Y} = v$. With this transformation the nominal control input $u_*(t)$ from (17) can also be given as

$$u_*(t) = U(\theta_*(t), \dot{\theta}_*(t)) = -\frac{R(\theta_*(t), 0, \dot{\theta}_*(t), 0)}{N(\theta_*(t), 0)}, \quad (42)$$

C. Integral of the reduced dynamics

The solution of a scalar second order differential equation of the form (18) is given by the integral function [5]

$$I^{(i)}(\theta, \dot{\theta}, \theta_0, \dot{\theta}_0) = \dot{\theta}^2 - \Psi(\theta_0, \theta) \left[\dot{\theta}_0^2 + \int_{\theta_0}^{\theta} \Psi(s, \theta) \frac{2\gamma(s)}{\alpha(s)} ds \right], \quad (43)$$

with

$$\Psi(\theta_1, \theta_2) = \exp \left\{ -2 \int_{\theta_1}^{\theta_2} \frac{\beta(\tau)}{\alpha(\tau)} d\tau \right\}, \quad (44)$$

which strictly preserves its zero value along a solution $\theta_*(t)$, initiated at $(\theta_0, \dot{\theta}_0) = (\theta_*(0), \dot{\theta}_*(0))$.

D. Coordinates measuring the distance

The dynamical system (40), possesses a natural choice of $(2n - 1)$ so-called transverse coordinates

$$x_{\perp} = [I^{(i)}(\theta, \dot{\theta}, \theta_{\star}(0), \dot{\theta}_{\star}(0)), Y, \dot{Y}]^T, \quad (45)$$

with $I^{(i)}(\cdot)$ being the scalar function (43)-(44) associated with the equation (18). The integral function qualifies as a transverse coordinate since it represents a robust method to quantify the distance from any given point to the desired trajectory [5]. Thus, the nonlinear dynamical system (40) presents a trivial solution defined for $t \in [0, T_e]$, and given by

$$Y \equiv 0, \quad \theta \equiv \theta_{\star}(t), \quad v \equiv 0. \quad (46)$$

E. Transverse Linearization

The linearization of the dynamics transverse to the motion (45) in the equilibrium (46) is defined by the linear time variant system

$$\frac{d}{d\tau}[\delta x_{\perp}] = A(\tau)\delta x_{\perp} + B(\tau)\delta v, \quad \tau \in [0, T]. \quad (47)$$

Exponential orbital feedback stabilization will be achieved using a solution of the continuous time-periodic dynamic Riccati equation

$$\begin{aligned} \dot{R}(\tau) + A(\tau)^T R(\tau) + R(\tau)A(\tau) + Q &= \\ R(\tau)B(\tau)\Gamma^{-1}B(\tau)^T R(\tau), & \end{aligned} \quad (48)$$

with appropriately chosen weighting matrices $Q \geq 0$ and $\Gamma > 0$.

The feedback control law

$$v(t) = -\Gamma^{-1}B(\tau)^T R(\tau)x_{\perp} \quad (49)$$

guarantees convergence for the nonlinear system within a vicinity of the desired trajectory. This controller can be implemented as presented in [7], [9], [10].

VI. SIMULATION RESULTS

For the purpose of demonstration, we have chosen the orbit depicted in bold line in Fig. 4, to exemplify oscillations around the horizontal equilibrium. This particular orbit has the initial conditions $\theta_0 = -0.24$, $\dot{\theta} = 0$, and a period $T = 0.4643$ sec. The nominal input computed from (17) is presented in Fig. 6. The validity of the inequality (12) corresponding to the normal reaction force is presented in the right of Fig. 6.

To exemplify oscillations around upright equilibrium we have chosen the orbit depicted in bold line in Fig. 5, This particular orbit has the initial conditions $\theta_0 = 1.35$, $\dot{\theta} = 0$, and a period $T = 0.432$ sec. The nominal input computed from (17) is presented in Fig. 7. The validity of the inequality (12) corresponding to the normal reaction force is presented in the right of Fig. 7.

To evaluate the performance of the controllers, we simulate the model with all our design parameters, but varying the initial conditions and introducing noisy disturbance in the output of the generalized coordinates, representing hardware uncertainty. As visualized in left side of Figs. 8, 9, the

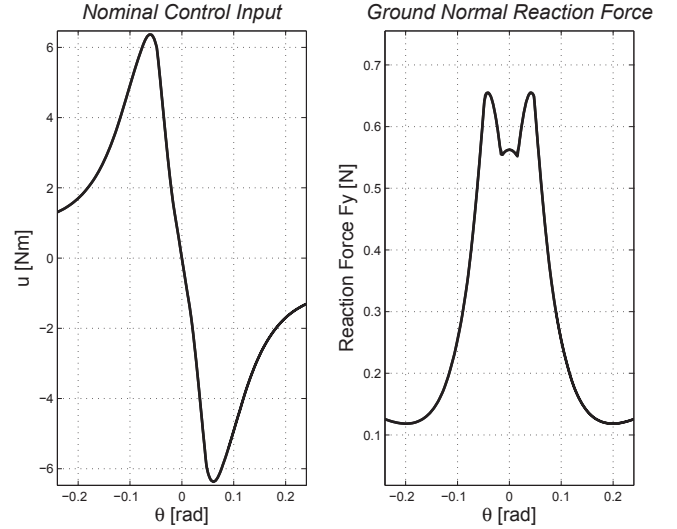


Fig. 6: Left: Nominal input as a function of θ using an arctangent constraint function. Right: Normal force as a function of θ using an arctangent constraint function

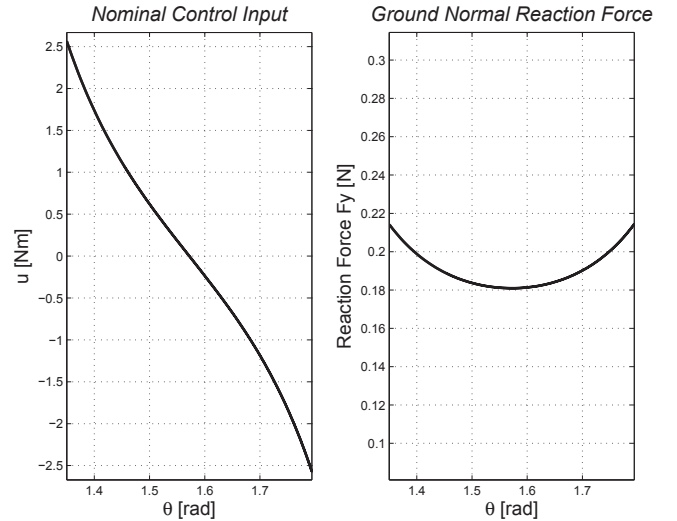


Fig. 7: Left: Nominal input as a function of θ using a linear constraint function. Right: Normal force as a function of θ using a linear constraint function

controller is able to converge to the desired cycle, and sustain a final periodic behavior. To verify this statement, we can refer to right side Figs. 8, 9, which shows the convergence of the transverse coordinates (45) to the equilibrium (46).

VII. CONCLUSIONS

We have considered the problem of planning and stabilizing periodic motions in a butterfly-shaped like robot. The main objective is to achieve the dynamic non-prehensile manipulation of a ball, resembling some of the complex motions performed by jugglers. Our aim is to provide analytical methods to approach such a problem for underactuated mechanical systems. Here, we have provided the preliminary analytical steps to achieve exponentially stable cycles around horizontal and vertical equilibria, that have been studied to realize experimental tests. These results have been analyzed

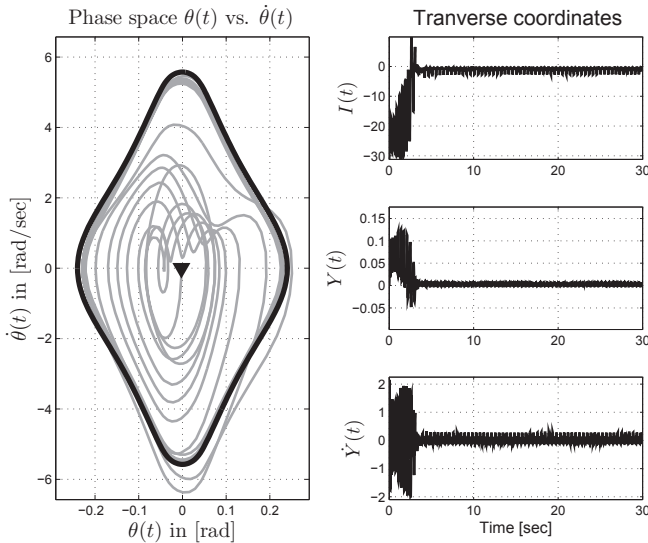


Fig. 8: Left: Convergence to the desired orbit, the initial condition is depicted by ∇ . Right: Convergence of transverse coordinates to the equilibrium (46)

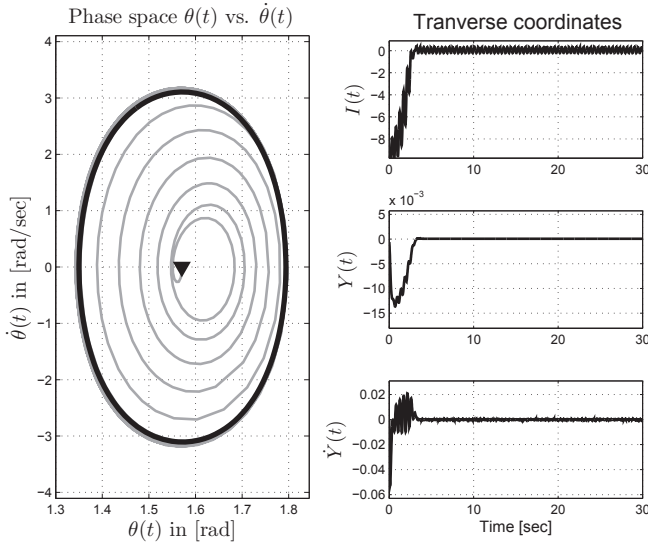


Fig. 9: Left: Convergence to the desired orbit, the initial condition is depicted by ∇ . Right: Convergence of transverse coordinates to the equilibrium (46)

by simulation studies, which allow us to validate the design concept, and assess all difficulties prior real-time implementation.

A. Acknowledgments

We would like to thank to Dr. Massimo Cefalo from "Sapienza University of Rome". We also thank Dr. Uwe Mettin for all his valuable comments and suggestions for this study.

REFERENCES

[1] K. Lynch, N. Shiroma, H. Arai, and K. Taine, "The roles of shape and motion in dynamic manipulation: The butterfly example," in *Proceedings of IEEE International Conference on Robotics and Automation (ICRA)*, 1998.

[2] M. Cefalo, L. Lanari, and G. Oriolo, "Energy-based control of the butterfly robot," in *Proceedings of the 3rd IFAC workshop on Periodic Control Systems*, 2006.

[3] M. Cefalo, *Controllo energy-based dei sistemi meccanici sottoattuati con applicazione al sistema Butterfly*. PhD thesis, Universita Degli Studi di Roma "La Sapienza", 2005.

[4] C. Canudas-de-Wit, B. Espiau, and C. Urrea, "Orbital stabilization of an underactuated three-link planar robot," in *Proceedings of the 15th IFAC World Congress*, (Barcelona, Spain), Jul. 21-26 2002.

[5] A. Shiriaev, J. Perram, and C. Canudas-de-Wit, "Constructive tool for orbital stabilization of underactuated nonlinear systems: Virtual constraints approach," *IEEE Transactions on Automatic Control*, vol. 50, no. 8, pp. 1164–1176, 2005.

[6] L. Freidovich, A. Shiriaev, F. Gomez-Estern, F. Gordillo, and J. Aracil, "Modification via averaging of partial-energy-shaping control for orbital stabilization: cart-pendulum example," *Int. J. Control*, vol. 82, no. 9, pp. 1582–1590, 2009.

[7] L. Freidovich, A. Robertsson, A. Shiriaev, and R. Johansson, "Periodic motions of the Pendubot via virtual holonomic constraints: Theory and experiments," *Automatica*, vol. 44, no. 3, pp. 785–791, 2008.

[8] L. Consolini and M. Maggiore, "Virtual holonomic constraints for euler-lagrange systems," in *Symposium on Nonlinear Control Systems (NOLCOS)*, 2010.

[9] P. L. Hera, L. Freidovich, A. Shiriaev, and U. Mettin, "New approach for swinging up the furuta pendulum: Theory and experiments," *Mechatronics*, vol. 19, no. 8, pp. 1240–1250, 2009.

[10] L. B. Freidovich, P. La Hera, U. Mettin, A. Robertsson, A. S. Shiriaev, and R. Johansson, "Shaping stable periodic motions of inertia wheel pendulum: theory and experiment," *Asian journal of control*, vol. 11, no. 5, pp. 548–556, 2009.

[11] CNRS – French National Center for Scientific Research, "Biped robot RABBIT." URL: <http://robot-rabbit.lag.ensieg.inpg.fr/English/>, accessed on 2007-08-18.

[12] J. Grizzle, G. Abba, and F. Plestan, "Asymptotically stable walking for biped robots: Analysis via systems with impulse effects," *IEEE Transactions on Automatic Control*, vol. 46, no. 1, pp. 51–64, 2001.

[13] E. Westervelt, J. Grizzle, C. Chevallereau, J. Choi, and B. Morris, *Feedback Control of Dynamic Bipedal Robot Locomotion*. CRC Press, Taylor and Francis Group, 2007.

[14] C. Nielsen, C. Fulford, and M. Maggiore, "Path following using transverse feedback linearization: Application to a maglev positioning system," *Automatica*, vol. 46, no. 3, pp. 585–590, 2010.

[15] M. Spong, S. Hutchinson, and M. Vidyasagar, *Robot Modeling and Control*. New Jersey: John Wiley and Sons, 2006.

[16] L. Freidovich, A. Shiriaev, and I. Manchester, "Stability analysis and control design for an underactuated walking robot via computation of a transverse linearization," in *Proceedings of the 17th IFAC World Congress*, (Seoul, Korea), Jul. 6-11 2008.

[17] A. Shiriaev and L. Freidovich, "Transverse linearization for impulsive mechanical systems with one passive link," *IEEE Trans. on Automatic Control*, vol. 54, no. 12, pp. 2882–2888, 2009.

[18] A. Shiriaev, L. Freidovich, and S. Gusev, "Transverse linearization for controlled mechanical systems with several passive degrees of freedom," *Automatic Control, IEEE Transactions on*, vol. 55, no. 4, pp. 893–906, 2010.